

# BEARZ Attack FALCON: Implementation Attacks with Countermeasures on the FALCON Signature Scheme

Sarah McCarthy<sup>1</sup>, James Howe<sup>2,†</sup>, Neil Smyth<sup>3,‡</sup>, Séamus Brannigan<sup>1</sup> and Máire O’Neill<sup>1</sup>

<sup>1</sup>Centre for Secure Information Technologies (CSIT), Queen’s University Belfast, U.K.

<sup>2</sup>PQShield Ltd., Oxford, U.K.

<sup>3</sup>Allstate NI, Belfast, U.K.

**Keywords:** Lattice-based Cryptography, Fault Attacks, FALCON, Digital Signatures, Post-quantum Cryptography, BEARZ, Countermeasures.

**Abstract:** Post-quantum cryptography is an important and growing area of research due to the threat of quantum computers, as recognised by the National Institute of Standards and Technology (NIST) recent call for standardisation. FALCON is a lattice-based signature candidate submitted to NIST, which has good performance but lacks in research with respect to implementation attacks and resistance. This research proposes the first fault attack analysis of FALCON and finds its lattice trapdoor sampler is as vulnerable to fault attacks as the GPV sampler used in alternative signature schemes. We simulate the post-processing component of this fault attack and achieve a 100% success rate at retrieving the private-key. This research then proposes an evaluation of countermeasures to prevent this fault attack and timing attacks of FALCON. We provide cost evaluations on the overheads of the proposed countermeasures which shows that FALCON has only up to 30% deterioration in performance of its key generation, and only 5% in signing, compared to runtimes without countermeasures.

## 1 INTRODUCTION

Digital signature schemes are an important cryptographic primitive, used for data authentication, integrity, and non-repudiation across the Internet and in secure computer systems. However, the discovery of Shor’s algorithm (Shor, 1999) has the potential to break all currently used signature schemes, such as ECDSA. This threat has led to a new era of cryptography which is built to withstand quantum computing attacks, known as post-quantum, or quantum-safe, cryptography. This threat has also prompted a standardisation effort by NIST (2016a) through their call for quantum-safe primitives. One of the most promising types of post-quantum solutions is lattice-based cryptography, which makes up almost half of the round 2 candidates. Many problems based on lattice assumptions provide the appealing property of worst-case to average-case hardness (Ajtai and Dwork, 1997) and lattices have yet to be hindered by

a serious cryptanalytic break. They also benefit from extended functionality, with primitives such as fully-homomorphic encryption (Gentry and Boneh, 2009) and identity-based encryption (Ducas et al., 2014).

This research focuses on lattice-based signatures, which have been shown to perform well in comparison to classical signature schemes (Howe et al., 2015). They also have relatively small key sizes, offer cryptographic agility, and most importantly offer protection from quantum attacks. There are three lattice-based signatures in round 2 of the NIST standardisation process, and we analyse the performance and attack resistance of one of these, FALCON (Prest et al., 2017).

Despite being resistant to quantum computing attacks, lattice-based cryptographic schemes are susceptible to the same side-channel attacks as alternative primitives used today, as summarised by Hodggers et al. (2016) and Khalid et al. (2018). Thus, considering attacks and possible countermeasures is important during standardisation and implementation. This research focuses on countermeasures of types of attack that have been considered to date for lattice-based signatures, namely timing and fault analysis attacks. Examples of these types of attacks and countermea-

<sup>†</sup>Most of this research was completed while the author was at the University of Bristol.

<sup>‡</sup>Most of this research was completed while the author was at the Centre for Secure Information Technologies (CSIT), Queen’s University Belfast.

tures are given in (Roy et al., 2014; Bruinderink et al., 2016; Howe et al., 2016; Espitau et al., 2016; Bindel et al., 2016; Karmakar et al., 2018).

This research considers timing and fault attacks and countermeasures of the lattice-based signature FALCON, including the first fault attack on the scheme. This is an important contribution to the NIST standardisation effort, as NIST (2016b) have stressed for the need for side-channel analysis (SCA) and efficient countermeasures. In NIST’s report on the second round candidates (Alagic et al., 2019), their comments for FALCON were that “more work is needed to ensure that the signing algorithm is secure against side-channel attacks” and this is the gap we hope to address in this paper. We review existing implementation attacks, propose the first fault attack on FALCON, and implement the signature scheme with appropriate countermeasures in place. The impact on performance with these countermeasures is thus also provided. The proposed attack, BEARZ, is a modification of the attack on the DLP (Ducas et al., 2014) hash-and-sign scheme by Espitau et al. (Espitau et al., 2016) (Espitau et al., 2018). The origins of FALCON are somewhat based on DLP, but it employs a novel recursive form of the GPV sampler in the FFT domain. We find that the FALCON sampler is still vulnerable to fault attacks and we are able to retrieve the private-key; however we show that it still performs competitively with countermeasures in place, incurring only a 5% decrease in performance. The zero-check countermeasure is effective against the proposed fault attack, and causes a 16% decrease in performance on the high security parameter set. Furthermore, we compare our results to those of signature schemes Dilithium (Lyubashevsky et al., 2017) and BLISS-B (Ducas, 2014) with similar countermeasures applied.

The contributions of this paper are as follows:

- The first fault attack on FALCON using a Basis Extraction by Aborting Recursion or Zeroing (BEARZ) technique.
- Novel portable ANSI C design of FALCON, with competitive performance (as part of libSAFE-crypto<sup>1</sup>). Features include constant-time components and use of the CDT (Gaussian) sampler.
- The first proposed design of FALCON with countermeasures against known side-channel attacks.
- A thorough overhead bench marking and comparison of FALCON with alternative state of the art signature schemes incorporating side-channel countermeasures.

<sup>1</sup><https://github.com/safecrypto/libsafecrypto>

The structure of the paper is as follows. Section 2 introduces lattice-based cryptography and describes the signature schemes discussed in this research. Section 3 outlines timing attacks on FALCON and proposed countermeasures. Section 4 presents the first fault attack on FALCON, followed by appropriate countermeasures to prevent this attack. Section 5 presents performance figures for our software implementations of the signature scheme, with and without attack countermeasures, followed by evaluations. The paper is then concluded in Section 6.

## 2 LATTICE-BASED DIGITAL SIGNATURE SCHEMES

This section describes preliminaries on lattice-based cryptography and introduces the FALCON signature scheme (Prest et al., 2017) and its relation to the DLP IBE (Ducas et al., 2014) scheme.

### 2.1 Preliminaries

Lattices are specified by a collection of vectors,  $x_i$ , which form their basis,  $\mathcal{B}$ , which can be defined as:  $\mathcal{L}(\mathcal{B}) = \{\sum_i a_i x_i | a_i \in \mathbb{Z}, x_i \in \mathcal{B}, 1 \leq i \leq n\}$ . Computationally hard lattice problems, such as the Shortest Vector Problem (SVP), Short Integer Solution (SIS), and Learning With Errors (LWE) (Regev, 2005, 2009) can form security assumptions for cryptographic primitives. In this research, we examine schemes which use *module* or *ideal* lattices, which progressively add more structure to the basis. The hardness assumption of FALCON’s key generation is based on a variant of the NTRU problem, which states that, given polynomial ring element  $A = g \cdot f^{-1}$ , it is difficult to recover  $f$  and  $g$ . The hardness of the signing procedure depends on the SVP, which states that if we are given the public basis of the lattice, it is a hard to find a short vector in the lattice.

We denote by  $N$  the dimension of the ring,  $q$  the modulus, and we operate in the polynomial ring  $\mathcal{R}_q = \mathbb{Z}_q[x]/(x^n + 1)$ . The elements in  $\mathcal{R}_q$  can be represented as polynomials of degree  $N$  or vectors of dimension  $N$ . These parameters for FALCON are given in Table 1, as well as the (equivalent) security levels of each parameter set.

### 2.2 The FALCON Signature Scheme

The FALCON signature scheme was proposed by Prest et al. (Prest et al., 2017). Its notable characteristics are that it is a hash-and-sign type signature

Table 1: The proposed parameters (Prest et al., 2017) for the FALCON signature scheme.

Parameter Set	NIST Level	Security Level	Dimension (N)	Modulus (q)
Set 1	Level 1	AES128	512	12289
Set 2	Level 4	SHA384	1024	12289
	Level 5	AES256	1024	12289

scheme (in contrast to Dilithium, a Fiat-Shamir signature scheme) and is secure in the random oracle model. It is based on the DLP identity-based encryption scheme proposed by Ducas et al. (2014), together with fast Fourier sampling techniques proposed Ducas and Prest (2016). These techniques improve the compactness of the private key and speed of the sampling procedure. The key generation process, shown in Algorithm 1, produces NTRU polynomials, where  $f$  and  $g$  become the private keys, and  $h = gf^{-1}$  is the public key. For the signing process, shown in Algorithm 2, the *ffSampling* algorithm (Algorithm 3) finds a short vector in the NTRU lattice, using the private key. The public key is used to verify the signature by checking the modulus lies beneath the required bound  $\beta$  in the verification algorithm, given in Algorithm 4.

### 2.3 The DLP Signature Scheme

Espitau et al. (2016, 2018) present an attack on the GPV-based DLP hash-and-sign signature scheme. In their fault model, the attacker is able to abort a loop early in the GPV Gaussian lattice-sampling stage in the signing algorithm. Whilst sampling vector coefficients of a signature polynomial of degree  $2n$ , they force the process to terminate at some iteration  $m \leq n$ , and obtain a faulty signature in the sub-lattice of rank  $m$ . After producing around  $m + 3$  faulty signatures, they can generate the original lattice and recover a short vector with probability 86%, thereby recovering enough of the NTRU lattice structure to obtain the private key. Espitau et al. recommend checking the validity of the DLP signature before sending, by running the verification algorithm. In Section 4, we construct a variant of this attack which targets the FALCON signature scheme.

## 3 TIMING ATTACKS ON FALCON

### 3.1 Gaussian Sampler

Gaussian samplers are used in FALCON to sample short lattice vectors. Generally in lattice-based

---

Algorithm 1: FALCON key generation (adapted from (Prest et al., 2017)).

---

**Data:**  $N, q$   
**Result:**  $\mathbf{B} \in \mathbb{Z}_q^{2N \times 2N}, h \in \mathcal{R}_q$

- 1  $\sigma_f = 1.17\sqrt{\frac{q}{2N}}$
- 2  $f, g, \leftarrow \mathcal{D}_{N, \sigma_f}$
- 3 Norm  
 $\leftarrow \max\left(\|g, -f\|, \left\|\left(\frac{q\bar{f}}{f^*f+g^*g}, \frac{q\bar{g}}{f^*f+g^*g}\right)\right\|\right)$
- 4 **if** Norm  $> 1.17\sqrt{q}$  **then** go to Step 2;
- 5 Compute  $\rho_f, \rho_g \in \mathcal{R}$  and  $R_f, R_g \in \mathbb{Z}$  such that:  $\rho_f \cdot f = R_f$  and  $\rho_g \cdot g = R_g$
- 6 **if**  $\text{GCD}(R_f, R_g) \neq 1$  or  $\text{GCD}(R_f, q) \neq 1$  **then** go to Step 2;
- 7 Compute  $u, v \in \mathbb{Z}$  such that:  
 $u \cdot R_f + v \cdot R_g = 1$
- 8  $F \leftarrow qv\rho_g$  and  $Q \leftarrow -qu\rho_f$
- 9  $k = \left\lfloor \frac{F^*f + G^*g}{f^*f + g^*g} \right\rfloor \in \mathcal{R}$
- 10  $F \leftarrow F - k^*f$  and  $G \leftarrow G - k^*g$
- 11  $h = g^*f^{-1} \text{mod } q$
- 12  $\mathbf{B} = \begin{pmatrix} g & -f \\ G & -F \end{pmatrix}$
- 13  $\hat{\mathbf{B}} = \begin{pmatrix} \text{FFT}(g) & -\text{FFT}(f) \\ \text{FFT}(G) & -\text{FFT}(F) \end{pmatrix}$
- 14  $\mathbf{T} = \text{ffLDL}^*(\mathbf{G})$
- 15  $\sigma \leftarrow 1.55\sqrt{q}$
- 16 for each leaf of  $\mathbf{T}$ , leaf.value =  $\sigma / \sqrt{\text{leaf.value}}$
- 17  $\text{sk} \leftarrow (\hat{\mathbf{B}}, \mathbf{T}), \text{pk} = h$
- 18 **return** sk, pk

---

cryptography, Gaussian samplers are known to be vulnerable to timing analysis attacks and constant-time samplers can be expensive. Bruinderink et al. (Bruinderink et al., 2016) proposed the first timing attack on a lattice-based signature scheme, BLISS, and recovered the private key by targeting the scheme’s Gaussian sampler. Because of this, there has been significant research on designing the Gaussian sampler to operate in independent time (Saarinen, 2015; Khalid et al., 2016; Howe et al., 2016; Micciancio and Walter, 2017).

---

 Algorithm 2: FALCON signing (adapted from (Prest et al., 2017)).
 

---

**Data:**  $sk, H : \{0, 1\}^* \rightarrow \mathbb{Z}_q^N, m, \beta$   
**Result:**  $SIG_m$

- 1 **if**  $SK_m$  is in local storage **then**
- 2     **return** Output  $SIG_m$  to message  $m$
- 3 **else**
- 4      $r \leftarrow \text{Unif}(\{0, 1\}^{320})$
- 5      $c \leftarrow H(r||m)$  ;
- 6      $t \leftarrow (\text{FFT}(c), \text{FFT}(0)) \cdot \hat{\mathbf{B}}^{-1}$   
        $z \leftarrow \text{ffSampling}(t, T)$
- 7      $s = (t - z)\hat{\mathbf{B}}$
- 8     **while**  $\|s\| > \beta$
- 9          $(s_1, s_2) \leftarrow \text{invFFT}(s)$
- 10         $s_2 = \text{Compress}(s_2)$
- 11         $SIG_m \leftarrow (r, s_2)$
- 12     **return** Output  $SIG_m$  associated to message  $m$  and keep in local storage

---



---

 Algorithm 3: ffSampling (Prest et al., 2017).
 

---

**Data:**  $\mathbf{t} = (t_0, t_1)$  in FFT format,  $T$   
**Result:**  $\mathbf{z} = (z_0, z_1)$  in FFT format

- 1 **if**  $n = 1$  **then**
- 2      $\sigma' \leftarrow T.\text{value}$
- 3      $z_0 \leftarrow \mathcal{D}_{\mathbb{Z}, t_0, \sigma'}$
- 4      $z_1 \leftarrow \mathcal{D}_{\mathbb{Z}, t_1, \sigma'}$
- 5     **return**  $\mathbf{z} = (z_0, z_1)$
- 6 **else**
- 7      $(l, T_0, T_1) \leftarrow (T.\text{value}, T.\text{leftchild}, T.\text{rightchild})$
- 8      $\mathbf{t}_1 \leftarrow \text{splitfft}(t_1)$
- 9      $\mathbf{z}_1 \leftarrow \text{ffSampling}(\mathbf{t}_1, T_1)$
- 10      $z_1 \leftarrow \text{mergefft}(\mathbf{z}_1)$
- 11      $t'_0 \leftarrow t_0 + (t_1 - z_1) \cdot l$
- 12      $\mathbf{t}_0 \leftarrow \text{splitfft}(t'_0)$
- 13      $\mathbf{z}_0 \leftarrow \text{ffSampling}(\mathbf{t}_0, T_0)$
- 14      $z_0 \leftarrow \text{mergefft}(\mathbf{z}_0)$
- 15     **return**  $\mathbf{z} = (z_0, z_1)$

---

### 3.2 Number Theoretic Transform

The NTT is commonly used in lattice-based cryptography, such as FALCON, to speed up multiplication of ring polynomials. However, it involves a lot of modular arithmetic, which is difficult to implement in constant-time, as described by Scott (2017), and so is a potential risk. There has also been significant research on attacking the NTT, as well as making the module run in constant-time (Longa and Naehrig, 2016; Alkim et al., 2016; Primas, 2017).

---

 Algorithm 4: FALCON verifying (adapted from (Prest et al., 2017)).
 

---

**Data:**  $pk = h \in \mathcal{R}_q, (SIG_m, m), \beta$   
**Result:** Accept or Reject

- 1  $c \leftarrow H(r||m)$
- 2  $s_2 = \text{Decompress}(s_2), s_1 \leftarrow c - s_2 h \pmod q$
- 3 **if**  $\|(s_1, s_2)\| < \beta$  and  $H(r||m) = c$  **then**
- 4     **return** Accept
- 5 **else**
- 6     **return** Reject

---

### 3.3 HashtoPoint

The HashtoPoint function hashes the message to a point in the polynomial ring. The authors of FALCON note that this “may be difficult to efficiently implement in a constant-time way”. If the message is to be kept secret, this could pose a problem.

### 3.4 Proposed Countermeasures to Timing Attacks

We now discuss existing countermeasures in the literature which we incorporate into our FALCON implementation, as well as novel designs of constant-time components.

Roy et al. (2014) introduced shuffling of the Gaussian-distributed vector as a countermeasure to timing attacks, which was also extended by Howe et al. (2016). The Fisher-Yates shuffling algorithm (Fisher et al., 1938) is typically used to effectively randomly permute these vector coefficients. However, Pessl (2016) suggested that this countermeasure is not sufficient on its own. The BlindVector algorithm introduced by Saarinen (2017) extended the use of the Fisher-Yates shuffling procedure to enhance random shuffles for side-channel protection. We utilise this algorithm and ensure a constant-time implementation to further increase the attack complexity. The algorithmic loops are not data dependent and the operations are such that regardless of whether a value is swapped or not they are always performed.

We introduce sample discard, the process whereby extra cache reads from random addresses are performed, in an attempt to distort statistics used in SCA. These extra reads are then thrown away. In this implementation, where it has been added as an extra preventative layer, we have used a range of discard rates at 6.25%, 12.5%, and 25%.

Our designs use a novel, efficient constant-time design of the CDT Gaussian sampling technique as this is much more simple to adapt for multiple parameter sets than other contenders. An exact number of

look-up reads are performed each time, with the comparison being computed using arithmetic logic using the same operations regardless of the branch which we want to take according to the CDT algorithm. The upper bound for the number of look-ups required is  $\lceil \log_2 N \rceil$  and so each call of the sampler is padded out to the nearest power-of-two to take this same amount of clock cycles. For the required values of the standard deviation, this CDT sampler gives better performance than the Knuth-Yao, discrete Ziggurat, and Bernoulli samplers when operated in constant-time.

The NTT and FFT functions are also made constant-time in our designs. The modular reduction part of NTT can leak timing information (Scott, 2017) and so our implementation is made constant-time by avoiding branch operations at the cost of some performance. This is done by processing all required branch variables and eschewing logic for more time consuming arithmetic operations. Performance is increased by employing lazy reduction to reduce the number of modular reductions that occur and using SIMD vectorisation. Point-wise modulo multiplication computes each element independently, allowing a multiplication of two polynomial rings in the NTT domain. As the operations are sequential and unconditional, it is constant-time.

The transform routinely utilises the Cooley-Tukey NTT algorithm with some small optimisations designed to increase performance, enable automatic vectorisation, and ensures that no conditional branch operations are used. The inverse NTT operation is the mirrored operation of the forward NTT, but additionally requires shuffling of the output coefficients and the use of both forward and inverse roots of unity coefficient tables. Automatic vectorisation of the final shuffle of the inverse NTT was not possible as the loop conditions were considered too complex and therefore it is performed separately to the modular reduction in order to improve performance. Our modular reduction design is a simplified range restriction that avoids the use of logical operations and instead opts to use arithmetic operations, in particular the constant time *less than* comparison function.

## 4 BEARZ ATTACK FALCON

This section proposes a new fault attack on the FALCON digital signature scheme, which uses Basis Extraction by Aborting Recursion or Zeroing, named BEARZ. The attack exerts and then exploits faults in the FALCON signature scheme in order to learn private key information, following a similar attack used on DLP. We utilise a different attack model, assuming

that the attacker is able to skip instructions and to zero variables as assumed by Bindel et al. (2016, 2017). The original attack is on the GPV sampling component in DLP, however there are two major differences between this sampler and the FALCON sampler: *recursion* and *FFT domain*.

### 4.1 DLP Attack

We begin with a recap of the attack on DLP by Espitau et al. (2016). In the GPV lattice trapdoor sampler, coefficients of the  $n$ -dimensional vectors  $(R, r)$  are sampled in a  $2n$ -length loop in reverse, from the last coefficient  $r_n$  to the first coefficient  $R_0$ . This is converted to a short Gaussian-distributed lattice vector by multiplying the vector  $(R, r)$  by the basis:

$$\mathcal{B} = \begin{pmatrix} \mathcal{A}(g) & -\mathcal{A}(f) \\ \mathcal{A}(G) & -\mathcal{A}(F) \end{pmatrix},$$

where  $\mathcal{A}(F)$  is the anti-circulant matrix associated with the degree- $n$  polynomial,  $F$ . We are concerned with second half of the signature, denoted  $s_2 = (R, r)(-\mathcal{A}(f), -\mathcal{A}(F)) = R \cdot f + r \cdot F$ , which is a  $2n$ -dimensional vector.

The fault attack is a loop abort on the  $2n$ -loop which samples the  $(R, r)$  coefficients. It causes the loop to abort at the  $m^{\text{th}}$  iteration, where  $m \leq n$ . This effectively eradicates the vector  $R$ , so  $s_2$  becomes:  $s_2 = (0, \dots, 0, r_0, \dots, r_{m-n})F$ , or alternatively the polynomial  $s_2 = r_0 x^{n-1} F + r_1 x^{n-2} F + \dots + r_{m-1} x^{n-m} F$ , which is in the sub-lattice of  $\mathcal{L}(\mathcal{A}(F))$ . With a certain number of faulty signatures,  $l \approx m$ , one will obtain a set spanning the lattice. From this, lattice reduction can be used to find a short vector, which should be one of the signed shifts of  $F$ , from which the private basis can be recovered. We now propose a similar attack which works for FALCON.

### 4.2 Recursion of FALCON

The FALCON sampling algorithm, shown in Algorithm 3, can be viewed as a recursive form of the GPV sampler. We change the attack notation to match that in FALCON's specifications (Prest et al., 2017), where  $(R, r)$  in the DLP scheme becomes  $z = (z_0, z_1)$ . The DLP attack inserts a loop abort fault at some iteration,  $m$ , of the  $2n$  loop (Espitau et al., 2016, Fig. 2), however in FALCON this translates to aborting the recursive call early (Prest et al., 2017, Alg. 18). To do this, we need to examine the structure of the recursion. There are two recursive calls in the top level of the *ffSampling* algorithm, given the target vector  $(t_0, t_1)$ , it acts first on  $t_1$ , recursively, from right to left, and then on  $t_0$ . Each of  $t_1$ , and then  $t_0$ , continuously splits into two vectors of length  $n := n/2$

until  $n = 2$ , and then samples the coefficients from a Gaussian distribution, before building back up to give sample vector  $(z_0, z_1)$ . Hence, there are two recursive branches within the top level algorithm. Also, this is all performed within the FFT domain. For a vector of length  $n$ , the first  $n/2$  values represent the real coefficients and the second  $n/2$  represent the imaginary coefficients. So, the initial approach would be to terminate the recursive call at the required point so that only  $m - n$  spaces would be filled, but this would not work due to the nature of the FFT functions.

### 4.3 FFT: Merging and Splitting

The sampling algorithm calls merging and splitting functions as subroutines. These functions do not simply break up and concatenate the polynomial ring elements. The split function separates a polynomial into its even and odd coefficients and is performed in the FFT domain. Operating in the FFT domain causes issues for the fault attack, since a zero input does not translate to zero in the FFT domain. Thus, we have to track the coefficients of the samples as they move up through the recursive tree of the algorithm. This is done by manually examining the pseudocode. Once the lattice vector has been obtained from the Gaussian sample, the  $\text{FFT}^{-1}$  function is applied to it, and the signing and verifying procedures are the same as in DLP. This means the same post-processing can be used from the DLP attack, however we need to ensure that the signature is not in the FFT domain by applying the inverse FFT function.

We now present different methods of attack, differentiated by the point at which the abortion occurs, this being the  $m$  positions from the end of the vector. This depends on where the attacker decides to abort the sample generation. All attack methods lead to the same output vector format for  $z$ ; the first  $(2n - m)$  coefficients of  $z = (z_0, z_1)$  are forced to zero.

#### 4.3.1 Abort Second Recursion (for $m = n$ )

This attack can be performed in a straightforward manner. Simply abort at the top sampling algorithm call, after the first recursive call, after Line 10 of Algorithm 3. Therefore  $z_1$  gets filled with sampled coefficients, yet  $z_0$  remains all zeros. This fault abortion is also performed for the case where  $m \leq n$ , in order to zero the first  $n$  coefficients.

#### 4.3.2 Zeroing or Skipping Attack (for $m \leq n$ )

There are two options for this attack. First, at the penultimate merge ( $n = 256$  to  $512$ ), set the required coefficients (e.g., the first half if  $m = n/2$ ) of the output coefficients to zero by skipping operations or later zeroing the corresponding coefficients. The skipped operations are  $f[(u \ll 1) + 0] = t\_re$  and  $f[(u \ll 1) + 1] = t\_re$ , from the reference code<sup>2</sup> (Prest et al., 2017). Otherwise, one can set the first required number of coefficients of  $z_1$  to zero before computing the corresponding lattice vector, that is, overwrite the sampler output  $z_1$ .

#### 4.3.3 Aborting Mid-recursion ( $m \leq n$ )

This attack is more sophisticated, as we must track the coefficients throughout the tree. Although this requires a prior one-off computation, it allows the fault to be applied at the one-dimensional Gaussian sampler stage, which is an easier point to physically exploit.

Suppose the target is  $m = n/2$ ; we want the left half of  $z_1$  to be zero. For this to occur, the left-hand side (LHS) vector in the final `merge_fft()` call has to have its first half equal to zero, and the right-hand side (RHS) vector has to have the first half of its coefficients equal to the second half. We generate each real coefficient (the first half) of the  $z_1$  vector by  $z_1[2u] = f_0[u] + (f_1[u] - f_1[u + n/4])$  and  $z_1[2u + 1] = f_0[u] - (f_1[u] - f_1[u + n/4])$ , where  $n$  is the dimension of the higher-level vector, and  $u \in \{0, \dots, n/4 - 1\}$ . Note that constants have been removed from the equations as they are irrelevant for the result.

For  $z_1[2u]$  and  $z_1[2u + 1]$  to be zero, we can set  $f_0[u] = 0$  and  $f_1[u] = f_1[u + n/4]$  for each  $u \in \{0, \dots, n/4 - 1\}$ . So for  $n = 512$ , the first  $n/4 = 128$  coefficients of the LHS 256-dimension vector are set to equal zero, and the first 128 coefficients of the RHS 256-dimension vector are set to equal the second 128 coefficients.

For the LHS 256-dimension vector, the first half of its coefficients must equal zero. The LHS 128-dimension vector must have its first half equal to zero, and the RHS 128-dimension vector must have the first half of its values equal to the second half of its values. This process is repeated on the LHS. The RHS 256-dimension vector must have the first half coefficients equal to the second half. For this to occur, the LHS 128-dimension vector must have the real values equal to the imaginary values, and the RHS 128-dimension vector must equal zero.

<sup>2</sup>Specifically, the `merge_fft()` function in `falcon_fft.c`

This conclusion is reached by considering the fact we want  $f[2u] = f[2u + n/2]$  (first real/imaginary computation per iteration) and  $f[2u + 1] = f[2u + 1 + \frac{n}{2}]$  (second real/imaginary) equal for each iteration of  $u$ .

From the `merge_fft()` function, this means  $f_0[u] + (f_1[u] - f_1[u + n/4]) = f_0[u + n/4] + (f_1[u] + f_1[u + n/4])$  and  $f_0[u] - (f_1[u] - f_1[u + n/4]) = f_0[u + n/4] - (f_1[u] + f_1[u + n/4])$ . To satisfy the components of the equations, we can set  $f_0[u] = f_0[u + n/4]$ , that is the first half of coefficients equal to second half, and for the second component, we can set  $f_1[u] = f_1[u + n/4] = 0$ . Therefore the equations will simply depend on the LHS feed-in vector.

For the RHS, every branch below can be set equal to zero. Take the LHS 128-dimension vector. It follows the same conditions as the level above, that is the LHS 64-dimension vector must have its real and imaginary values equal, and the RHS must be zero. Any vector equalling zero must have both feed-in vectors equalling zero, so the branches below this can be zeroed. This method can be applied for any  $m$  such that  $m = 2^k$ , where  $k \in \mathbb{Z}$ .

#### 4.4 Post-attack Processing

The final step of the attack involves recovery of the private basis from the faulty signatures. Suppose we have the first  $2n - m$  coefficients of vector  $(z_0, z_1)$  equal to zero. Then, according to the signing algorithm (Algorithm 2) of FALCON, we compute the signature  $s_2$  as:

$$s = t - z\hat{B},$$

where  $\hat{B}$  is the basis matrix in the FFT domain. But we only need the second half of  $s$ , that is  $s_2$ , where

$$s_2 = t_1 - z \begin{pmatrix} -\mathcal{A}(f) \\ -\mathcal{A}(F) \end{pmatrix},$$

and since  $t_1$  is set to zero,

$$s_2 = -z \begin{pmatrix} -\mathcal{A}(f) \\ -\mathcal{A}(F) \end{pmatrix}.$$

Furthermore, the first  $m - n$  coefficients of  $z$  are zero, which further implies:

$$s_2 = -z_1 (-\mathcal{A}(F)),$$

and since some of the coefficients of  $z_1$  are zero, we finally have:

$$s_2 = (z_1[m-1]x^{n-m}F + \dots + z_1[0]x^{n-1}F).$$

This leaves us with a sub-lattice of the lattice generated by  $F$ , akin to that obtained in the DLP attack.

The only difference is that we are in the FFT domain, which we overcome by applying the inverse FFT function to the output. Thus, with multiple faulty signatures, the lattice spanned by  $F$  (where  $F$  is a short vector in this lattice) can be found, where the BKZ algorithm can be used to retrieve it. Then  $G, f$ , and  $g$  can be deduced from the public key  $h$ , and thus the private NTRU lattice basis can be found.

#### 4.5 Attack Results

The aim of this research is to show that if this fault attack is applied successfully, the the output can reveal the private key. The technicalities of the fault injection are left as future work. Thus, to verify this attack model, we first tested each method of attack through software simulation and ensured the output signature gave the expected number of zeros. This was successful for all attack methods and parameter sets. We then collected  $l$  faulty signatures for the values of  $m$  zeros given in Table 2, and ran the BKZ algorithm (FPLLL Development Team, 2016) to obtain the private key polynomial  $F$ . The timings in seconds for the BKZ algorithm to obtain  $F$  are given in Table 2. The assumptions and attack model are similar to that used by Espitau et al. (2016), in particular for estimating the number of faults required.

#### 4.6 Fault Model

The physical attack methods required for BEARZ are early abortion and zeroing. Side-channel analysis may be used to detect the window between the first call and the second recursive call, within which the algorithm can be aborted, as in the original DLP attack. A zeroing attack can be performed as a memory-based attack, during storage of the vector in RAM, by setting the required bits to zero (Naccache et al., 2005). Alternatively, skipping lines of code can be performed by CPU clock glitching (Blömer et al., 2014). With respect to the fault models guide (Verbauwhede et al., 2011), we can classify the BEARZ fault attack models as being on the processing part (for zeroing) and program flow (for skipping and aborting). These are high precision attacks, where the adversary has the ability to bit flip/set, and targets the cryptographic primitive.

#### 4.7 Countermeasures to BEARZ

Bindel et al. (2017) discuss countermeasures relevant to BEARZ. A straightforward method of detecting fault attacks (such as by Bruinderink and Pessl

Table 2: Timings (in seconds) to run the BKZ algorithm on  $l$  faulty signatures to obtain the basis polynomial  $F$  running on a single core of an Intel Core i7-6700HQ CPU at 2.60 GHz.

Parameters	$m$	$l = m + 1$	$l = m + 2$	$l = m + 3$
Set 1	64	0.07	0.07	0.08
	128	0.35	0.30	0.36
	256	2.17	2.80	2.36
	385	10.9	12.8	11.8
Set 2	128	0.28	0.29	0.35
	256	2.24	2.55	2.67

(2018)) is to compute the signature twice. The double computation method works for non-deterministic schemes by fixing the randomness. A conservative estimate of this is doubling the signing time. Running the verification process immediately after signing can give the signer confidence that their hardware has not been subject to fault attacks (Bruinderink and Pessl, 2018). A simple, efficient method of detecting the BEARZ attack is checking that the sampled vector does not go to zero at some point along its length at the end of the *ffSampler* algorithm.

## 5 RESULTS AND EVALUATION

This section analyses the performance results of the optimised software design of the FALCON signature scheme, as well as the three countermeasures discussed in the previous section. Clearly, as with any attack countermeasure, we expect some performance degradation, however we are more concerned with their relative impacts on performance. Unless otherwise stated, performance figures were obtained on Intel E5-1620 CPU @ 3.7GHz, with hyperthreading disabled, running on a single CPU. The platform of the reference figures are also stated. Any results with “-” mean the results are unchanged, thus not being affected by the countermeasure(s).

Our libSAFEcrypto implementation consists of portable C code that is written to permit a compiler (gcc) to generate AVX-2 assembler (or any other type of SIMD code) without having to revert to writing assembler code by hand. It can also be ported to other target processors (like ARM) without having to re-write the code; this portability was set out as one of our major design goals in the project to provide for wide adoption. This portability comes at a performance cost, but is advantageous if one wants to support various systems (embedded or server), quickly adapt to changing algorithms (like a NIST post-quantum scheme), or are looking for wide support. Therefore our performance is lower than the reference implementation by Prest et al. (2017).

### 5.1 FALCON with Countermeasures

Results for our FALCON optimised designs and the effects of our countermeasures are shown in Table 3. Parameter sets for FALCON slightly changed for the second round of NIST’s post-quantum standardisation. Specifically, the second set of parameters, thus we have omitted these from our results and performance analysis and focus on parameter sets 1 and 2.

Interestingly, FALCON’s performance is not largely affected by the countermeasures. Applying verify-after-sign to protect against BEARZ does not significantly slow performance (~ 5%), and the key generation only drops significantly with a high sample discard rate. The recommended combination of countermeasures together slow the key generation and signing down by less than 5% for Parameter Set 1. Sample discard has less than a 5% effect on key generation, and the effect of the 6.5% rate on Parameter Set 1 is so minimal that the effect of fluctuation causes an increase from the rate without discard. This small effect on performance is due to the sampling and verification processes being efficient.

### 5.2 Effectiveness of Countermeasures

#### 5.2.1 Timing Attacks

To verify our timing attack countermeasure, we ran the signing procedure 100 times and found for Set 1, it fell within a range of 50 operations per second, and for Set 2 within 20 operations per second. This suggests it is effective against timing attacks.

#### 5.2.2 BEARZ Attack

If the same fault is successfully implemented twice, then double computation will not suffice. The verify-after-sign may not detect a fault attack which targets the sampling, this has been shown previously by Espitau et al. (2016), thus it still may produce a valid signature and go undetected. However, the zero-check countermeasure should detect the attack with 100%



Table 3: Performance results (ops/sec) for FALCON with SCA countermeasures, including % decrease in affected components, on Intel E5-1620 @ 3.7GHz unless otherwise stated.

Implementation	Parameters	KeyGen	Sign	Verify	% decrease
Reference (Prest et al., 2017) Intel Core i7-6567U @ 3.3GHz	Set 1	143	6081.9	37175.3	-
	Set 2	50.9	3072.5	17697.4	-
Baseline +constant-time NTT	Set 1	29.8	1484	29002	-
	Set 2	11.1	734	14366	-
+Verify-after-sign	Set 1	-	1412	-	5
	Set 2	-	699	-	5
+Zero-check	Set 1	-	1006	-	32
	Set 2	-	489	-	16
+Double Computation +Verify after sign	Set 1	-	706	-	52
	Set 2	-	350	-	76
+Sample Discard (Low) (6.25%)	Set 1	26.3	-	-	12
	Set 2	12.0	-	-	+8
+Sample Discard (Medium) (12.5%)	Set 1	24.9	-	-	16
	Set 2	10.2	-	-	8
+Sample Discard (High) (25%)	Set 1	27.7	-	-	7
	Set 2	8.0	-	-	28
+Fisher-Yates Shuffling	Set 1	23.87	-	-	20
	Set 2	10.9	-	-	2
+BlindVector	Set 1	27.03	-	-	9
	Set 2	8.7	-	-	49
+Verify-after-sign +Sample Discard (Low) (6.25%) +Fisher-Yates Shuffling	Set 1	29.0	1426	-	4
	Set 2	10.7	706	-	4

success rate. We therefore recommend this as a minimum, sufficient countermeasure.

### 5.3 Comparison to Other Lattice-based Signature Schemes

We compare our results to our implementation of Dilithium (Lyubashevsky et al., 2017) and Bliss-B (Ducas, 2014) signature schemes with countermeasures in place. Interestingly, the performance of FALCON is not as adversely affected as much as its NIST competitor scheme Dilithium when the verify-after-sign countermeasure is added, as shown in Figure 1b. Even at high security levels, it does not suffer as much of a slowdown as BLISS-B, shown in Figure 1a. This is due to the efficiency of the FALCON components. Similar countermeasures on Dilithium that prevent the fault attack proposed by Bruinderink and Pessl (2018), cause its performance to deteriorate by almost 20%. BLISS-B has a larger range of countermeasures available in order to protect against those proposed by Pessl et al. (2017), meaning the effect on performance can range between an additional 10% and 50%, depending on the instance. Dilithium has the advantage of being immune to Gaussian sam-

pler attacks, however its protection from the fault attacks by Bruinderink and Pessl (2018) remain an open problem. Its performance is slowed down by nearly 20% with countermeasures in place and has greater degradation than BLISS-B with a protected Gaussian sampler.

## 6 CONCLUSION

In this research, we have proposed a new attack on the FALCON signature scheme, BEARZ. We have shown that FALCON is vulnerable to fault attacks on its Gaussian sampler and so consideration of physical attacks should be addressed when implementing for real world use. We also provide possible countermeasures, including the verify-after-sign countermeasure, as the faulty signature will not pass the norm bound test, and the zero-check. Furthermore, we implement double computation, a costly but reliable method, assuming the attacker only has access to the hardware during one of the signing processes. Additionally, we review timing attack vulnerabilities and countermeasures and compare the impact on performance to other lattice-based schemes, deducing that FALCON is

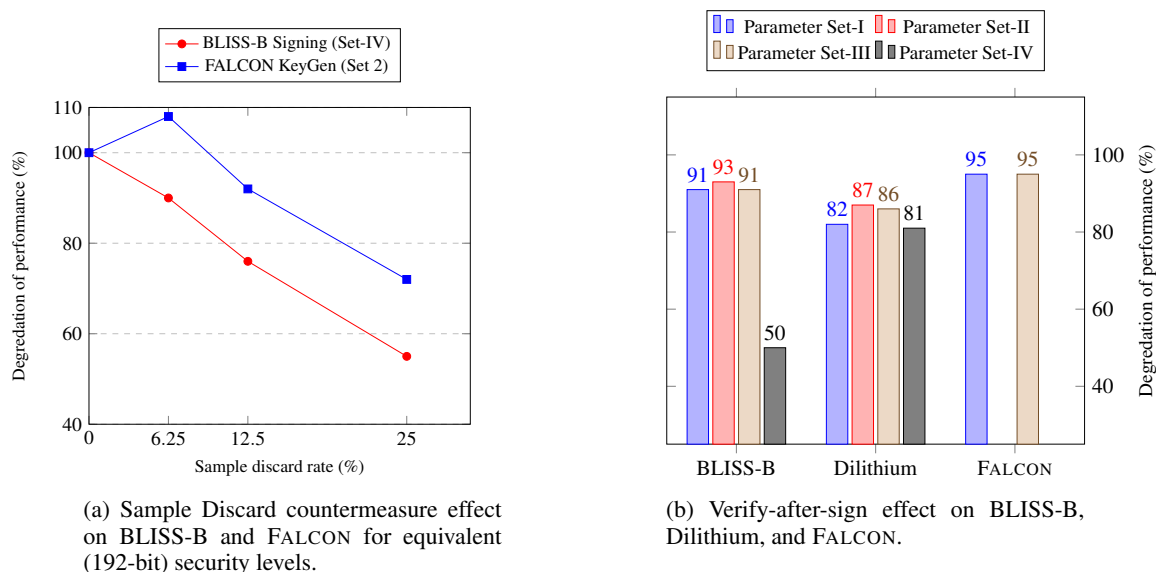


Figure 1: Performance analysis of the proposed SCA countermeasures for the FALCON, Dilithium, and BLISS-B signatures.

a still a competitive second-round candidate.

## ACKNOWLEDGEMENTS

The authors would like to thank Thomas Prest and the anonymous reviewers of T-CHES 2019 and COSADE 2019 for their careful reading of the paper and their diligent comments. The authors would also like to acknowledge that this work was supported in part by the European Union Horizon 2020 SAFEcrypto project (grant no. 644729) and the EPSRC via grant EP/N011635/1.

## REFERENCES

Ajtai, M. and Dwork, C. (1997). A public-key cryptosystem with worst-case/average-case equivalence. In *STOC '97 Proceedings of the twenty-ninth annual ACM symposium on Theory of computing*, pages 284–293.

Alagic, G., Alperin-Sheriff, J., Apon, D., Cooper, D., Dang, Q., Liu, Y.-K., Miller, C., Moody, D., Peralta, R., Perlner, R., Robinson, A., and Smith-Tone, D. (2019). Status Report on the First Round of the NIST Post-Quantum Cryptography Standardization Process. <http://aiweb.techfak.uni-bielefeld.de/content/bworld-robot-control-software/>. [Online; accessed February 2019].

Alkim, E., Ducas, L., Pöppelmann, T., and Schwabe, P. (2016). Post-quantum key exchange-a new hope. In *USENIX Security Symposium*, volume 2016.

Bindel, N., Buchmann, J., and Krämer, J. (2016). Lattice-based signature schemes and their sensitivity to fault

attacks. In *Fault Diagnosis and Tolerance in Cryptography (FDTC), 2016 Workshop on*, pages 63–77. IEEE.

Bindel, N., Kramer, J., and Schreiber, J. (2017). Special session: hampering fault attacks against lattice-based signature schemes-countermeasures and their efficiency. In *Hardware/Software Codesign and System Synthesis (CODES+ ISSS), 2017 International Conference on*, pages 1–3. IEEE.

Blömer, J., Silva, R. G. D., Günther, P., Krämer, J., and Seifert, J.-P. (2014). A practical second-order fault attack against a real-world pairing implementation. In *Fault Diagnosis and Tolerance in Cryptography (FDTC), 2014 Workshop on*, pages 123–136. IEEE.

Bruinderink, L. G., Hülsing, A., Lange, T., and Yarom, Y. (2016). Flush, Gauss, and reload-a cache attack on the BLISS lattice-based signature scheme. In *International Conference on Cryptographic Hardware and Embedded Systems*, pages 323–345. Springer.

Bruinderink, L. G. and Pessl, P. (2018). Differential fault attacks on deterministic lattice signatures. *IACR Transactions on Cryptographic Hardware and Embedded Systems*, pages 21–43.

Ducas, L. (2014). Accelerating BLISS: the geometry of ternary polynomials. Cryptology ePrint Archive, Report 2014/874. <https://eprint.iacr.org/2014/874>.

Ducas, L., Lyubashevsky, V., and Prest, T. (2014). Efficient identity-based encryption over ntru lattices. In *International Conference on the Theory and Application of Cryptology and Information Security*, pages 22–41. Springer.

Ducas, L. and Prest, T. (2016). Fast fourier orthogonalization. In *Proceedings of the ACM on International Symposium on Symbolic and Algebraic Computation*, pages 191–198. ACM.

Espitau, T., Fouque, P., G'erard, B., and Tibouchi, M. (2018). Loop-abort faults on lattice-based signature

- schemes and key exchange protocols. *IEEE Transactions on Computers*, 67(11):1535–1549.
- Esposito, T., Fouque, P.-A., Gérard, B., and Tibouchi, M. (2016). Loop-abort faults on lattice-based fiat-shamir and hash-and-sign signatures. In *International Conference on Selected Areas in Cryptography*, pages 140–158. Springer.
- Fisher, R. A., Yates, F., et al. (1938). Statistical tables for biological, agricultural and medical research. *Statistical tables for biological, agricultural and medical research*.
- FPLLL Development Team, O. T. (2016). fplll, a lattice reduction library. Available at <https://github.com/fplll/fplll>.
- Gentry, C. and Boneh, D. (2009). *A fully homomorphic encryption scheme*, volume 20. Stanford University Stanford.
- Hodgers, P., Regazzoni, F., Gilmore, R., Moore, C., and Oder, T. (2016). State-of-the-art in physical side-channel attacks and resistant technologies. *Technical report*.
- Howe, J., Khalid, A., Rafferty, C., Regazzoni, F., and O’Neill, M. (2016). On practical discrete Gaussian samplers for lattice-based cryptography. *IEEE Transactions on Computers*.
- Howe, J., Pöppelmann, T., O’Neill, M., O’Sullivan, E., and Güneysu, T. (2015). Practical lattice-based digital signature schemes. *ACM Transactions on Embedded Computing Systems (TECS)*, 14(3):41.
- Karmakar, A., Roy, S. S., Reparaz, O., Vercauteren, F., and Verbauwhede, I. (2018). Constant-time discrete gaussian sampling. *IEEE Transactions on Computers*.
- Khalid, A., Howe, J., Rafferty, C., and O’Neill, M. (2016). Time-independent discrete gaussian sampling for post-quantum cryptography. In *2016 International Conference on Field-Programmable Technology (FPT)*, pages 241–244. IEEE.
- Khalid, A., Oder, T., Valencia, F., O’Neill, M., Güneysu, T., and Regazzoni, F. (2018). Physical protection of lattice-based cryptography: Challenges and solutions. In *Proceedings of the 2018 on Great Lakes Symposium on VLSI*, pages 365–370. ACM.
- Longa, P. and Naehrig, M. (2016). Speeding up the number theoretic transform for faster ideal lattice-based cryptography. In *International Conference on Cryptology and Network Security*, pages 124–139. Springer.
- Lyubashevsky, V., Ducas, L., Kiltz, E., Lepoint, T., Schwabe, P., Seiler, G., and Stehle, D. (2017). CRYSTALS-Dilithium. Technical report, National Institute of Standards and Technology. available at <https://csrc.nist.gov/projects/post-quantum-cryptography/round-1-submissions>.
- Micciancio, D. and Walter, M. (2017). Gaussian sampling over the integers: Efficient, generic, constant-time. In *Annual International Cryptology Conference*, pages 455–485. Springer.
- Naccache, D., Nguyen, P. Q., Tunstall, M., and Whelan, C. (2005). Experimenting with Faults, Lattices and the DSA. In *International Workshop on Public Key Cryptography*, pages 16–28. Springer.
- NIST (2016a). Post-quantum crypto project. <http://csrc.nist.gov/groups/ST/post-quantum-crypto/>.
- NIST (2016b). Submission requirements and evaluation criteria for the post-quantum cryptography standardization process. <https://csrc.nist.gov/csrc/media/projects/post-quantum-cryptography/documents/call-for-proposals-final-dec-2016.pdf>.
- Pessl, P. (2016). Analyzing the shuffling side-channel countermeasure for lattice-based signatures. In *International Conference in Cryptology in India*, pages 153–170. Springer.
- Pessl, P., Bruinderink, L. G., and Yarom, Y. (2017). To BLISS-B or not to be: Attacking strongSwan’s Implementation of Post-Quantum Signatures. In *Proceedings of the 2017 ACM SIGSAC Conference on Computer and Communications Security*, pages 1843–1855. ACM.
- Prest, T., Fouque, P.-A., Hoffstein, J., Kirchner, P., Lyubashevsky, V., Pornin, T., Ricosset, T., Seiler, G., Whyte, W., and Zhang, Z. (2017). Falcon. Technical report, National Institute of Standards and Technology. available at <https://csrc.nist.gov/projects/post-quantum-cryptography/round-1-submissions>.
- Primas, R. (2017). Side-channel attacks on efficient lattice-based encryption. Master’s thesis, Graz University of Technology, Graz.
- Regev, O. (2005). On lattices, learning with errors, random linear codes, and cryptography. In *Proceedings of the 37th Annual ACM Symposium on Theory of Computing, Baltimore, MD, USA, May 22–24, 2005*, pages 84–93.
- Regev, O. (2009). On lattices, learning with errors, random linear codes, and cryptography. *Journal of the ACM (JACM)*, 56(6):34:1–34:40.
- Roy, S. S., Reparaz, O., Vercauteren, F., and Verbauwhede, I. (2014). Compact and side channel secure discrete Gaussian sampling. *IACR Cryptology ePrint Archive*, 2014:591.
- Saarinen, M.-J. O. (2015). Gaussian sampling precision and information leakage in lattice cryptography. *IACR Cryptology ePrint Archive*, 2015:953.
- Saarinen, M.-J. O. (2017). Arithmetic coding and blinding countermeasures for lattice signatures. *Journal of Cryptographic Engineering*, pages 1–14.
- Scott, M. (2017). A note on the implementation of the number theoretic transform. In *IMA International Conference on Cryptography and Coding*, pages 247–258. Springer.
- Shor, P. W. (1999). Polynomial-time algorithms for prime factorization and discrete logarithms on a quantum computer. *SIAM Review*, 41(2):303–332.
- Verbauwhede, I., Karaklajic, D., and Schmidt, J.-M. (2011). The fault attack jungle—a classification model to guide you. In *2011 Workshop on Fault Diagnosis and Tolerance in Cryptography*, pages 3–8. IEEE.